Oncogene. Author manuscript; available in PMC 2016 December 12.

Published in final edited form as:

Oncogene. 2015 August 06; 34(32): 4238–4247. doi:10.1038/onc.2014.357.

Coiled-coil domain containing 68 (CCDC68) demonstrates a tumor suppressive role in pancreatic ductal adenocarcinoma

Nikolina Radulovich[1,2], **Lisa Leung**[1,3], **Emin Ibrahimov**[1], **Roya Navab**[1], **Shingo Sakashita**[1], **Chang-Qi Zhu**[1], **Ethan Kaufman**[1], **William W. Lockwood**[4], **Kelsie L. Thu**[4], **Yaroslav Fedyshyn**[5], **Jason Moffat**[5], **Wan L. Lam**[4], and **Ming-Sound Tsao**[1,2,3]

[1]Princess Margaret Cancer Center, University Health Network, Toronto, Ontario, Canada

[2]Department of Laboratory Medicine and Pathobiology Department, University of Toronto, Ontario, Canada

[3]Department of Medical Biophysics, University of Toronto, Ontario, Canada

[4]British Columbia Cancer Research Centre and Department of Pathology, University of British Columbia, Vancouver, BC, Canada

[5]Department of Molecular Genetics, Banting & Best Department of Medical Research, University of Toronto, ON, Canada

Abstract

Using integrative genomics and functional screening we identified coiled-coil domain containing 68 (*CCDC68*) as a novel putative tumor suppressor (TSG) in pancreatic ductal adenocarcinoma (PDAC). *CCDC68* allelic losses were documented in 48% of primary PDAC patient tumors, 50% of PDAC cell lines, and 30% of primary patient derived xenografts. We also discovered a SNP variant (SNP rs1344011) that leads to exon skipping and generation of an unstable protein isoform $CCDC68\Delta^{69–114}$ in 31% of PDAC patients. Overexpression of full length *CCDC68* ($CCDC68^{wt}$) in PANC-1 and Hs.766T PDAC cell lines lacking *CDCC68* expression decreased proliferation and tumorigenicity in *scid* mice. In contrast, downregulation of endogenous *CCDC68* in MIAPaca-2 cells increased tumor growth rate. These effects were not observed with the deletion-containing isoform, $CCDC68\Delta^{69–114}$. In conclusion, our results suggest that *CCDC68* is a novel candidate TSG in PDAC.

Keywords

CCDC68; integrative genomics; pancreatic adenocarcinoma; tumor suppressor; alternative splicing; MAPK signalling; primary patient xenograft models

Corresponding author: Dr. Ming-Sound Tsao, Princess Margaret Cancer Center, 610 University Avenue, Toronto, Ontario, M5G 2M9, Ph.416-946-2000 ext.5617; Fax.416-946-2079. ming.tsao@uhn.on.ca.

Conflict of interest: The authors declare no conflict of interest.

Supplementary Information accompanies the paper on the *Oncogene* website (http://www.nature.com/onc)

Introduction

Pancreatic adenocarcinoma (PDAC) is the fourth leading cause of cancer-related death in North America, with a poor overall 5-year survival rate of only 5% (1). To date, no chemotherapeutic treatments have been found to be effective against this lethal disease.

Aside from a small percentage of familial cases, PDAC is driven by the accumulation of somatic alterations. Both the loss of tumor suppressor genes (TSGs) and activation of oncogenes are involved in pancreatic carcinogenesis. Key events in pancreatic carcinogenesis that have been validated as high-frequency alterations include *KRAS* activating mutations and inactivation of *CDKN2A, SMAD4* and *p53* TSGs (2). However, recent genome-wide surveys have demonstrated significant genetic heterogeneity among PDAC patients, with the occurrences of rare somatic mutations in many genes (3–5). Although many of the catalogued genetic alterations can be linked to one of 12-core cancer signaling pathways, experimental evidence to verify these novel alterations as either drivers of pancreatic carcinogenesis or passengers is still lacking. In this context, we have combined integrative analysis of genome/transcriptome data with functional shRNA and ORFeome screens to identify *CCDC68* as a putative TSG in PDAC.

Results

Integrative genomic analysis reveals *CCDC68* as a putative TSG in PDAC

We have previously shown that the immortalized near-normal human pancreatic duct epithelial (HPDE) cell line H6c7, when transformed by $KRAS^{G12V}$ oncogene (H6c7-Kr), gives rise to sporadic tumors when implanted into *scid* mice (6). However, H6c7-KrasT cell line re-derived from one of these tumors, could now produce tumors in *scid* mice with 100% efficiency. We hypothesized that additional genetic alterations arose in the H6c7-KrasT cell line, which synergized with $KRAS^{G12V}$ oncogene to cause the full malignant transformation of H6c7 cells into invasive carcinoma. To identify genetic alterations in H6c7-KrasT cells, whole-genome tiling path array comparative genomic hybridization (aCGH) was used to compare DNA copy number between H6c7-KrasT and H6c7-Kr cells. To select for true events, only alterations with the same status in both replicates and encompassing two adjacent clones were considered. Alterations in 11 genomic regions on 9 chromosome arms were identified (Supplementary Fig. S1). The main regions included losses on chromosome 8, 15q and 18q. These regions mapped to 221 genes with gain and 2342 genes with loss.

To identify the most probable TSGs involved in the transformation of H6c7-Kr into H6c7-KrasT cells we utilized integrative genomic analysis (Fig. 1A). Firstly, aCGH data was integrated with aCGH and transcriptome data from 20 established PDAC cell lines (7). The aCGH data were segmented to determine the copy number status (gain, loss or neutral) for each gene in each cell line. Then, the expression of each gene was compared between the altered and neutral samples using the Mann-Whitney U test. Genes whose expression was in the direction predicted by the copy number change and had a p-value<0.05 were considered significant. This analysis identified 206 genes lost and underexpressed in 20 PDAC lines relative to H6c7 (Supplementary TableS1). Further analysis revealed 5/206 genes (CCDC68, ARHGEF10, POLI, ME2 and CLN8) with mutation or homozygous deletion in primary

PDAC patients (3) and decreased mRNA expression in at least 30% of PDAC cell lines as compared to H6c7 cells (Fig. 1A). One of the identified genes, coiled-coil domain containing 68 (*CCDC68*) was further investigated as a putative TSG in PDAC (bottom panel: Fig. 1A).

CCDC68 expression negatively affects the growth of PDAC cell lines

We assessed the proliferative effects of *CCDC68* knockdown (H6c7-Kr and MIAPaca-2) and *CCDC68* open reading frame (ORF) overexpression (PANC-1 cells) in PDAC cell lines using the MTS assay. While decreased *CCDC68* levels significantly increased proliferation of H6c7-Kr and MIAPaca-2 cells, overexpression of *CCDC68* significantly decreased proliferation of PANC-1 cells (Fig. 1B). Using the xCELLigence platform, we confirmed the increased growth rate of MIAPaca-2 cells upon *CCDC68* knockdown (Fig. 1C) and decreased growth rate of PANC-1 cells expressing *CCDC68*ORF (Fig. 1D). Furthermore, the exogenous expression of *CCDC68* significantly decreased soft agar colony formation of PANC-1 cells (Fig. 1E).

CCDC68 expression decreases tumorigenicity of PDAC cell lines

CCDC68 was overexpressed in H6c7-KrasT, PANC-1 and Hs.766T cell lines containing undetectable endogenous *CCDC68* protein (top panel: Fig. 2A,B,C) and the resulting cell lines and those derived from vector-only controls were injected into subcutaneous tissue of *scid* mice to assess tumor growth rates (Fig. 2A,B,C). Overexpression of *CCDC68*ORF in H6c7-KrasT cells completely abrogated their ability to grow tumors in mice (Fig. 2A). Furthermore, our results revealed that overexpressing *CCDC68* significantly attenuated tumor growth in PANC-1 and Hs.766T xenograft models (Fig. 2B,C). The decreased tumor sizes in PANC-1 and Hs.766T xenograft models overexpressing *CCDC68* were also confirmed at necropsy (Supplementary Fig. S2).

We also downregulated *CCDC68* in MIAPaca-2 cells which express *CCDC68* endogenously, using two independent shRNAs targeting the 3′UTR region of the *CCDC68* mRNA (top panel: Fig. 2C). The resulting cell lines were subjected to *in vivo* tumorigenicity assays. Downregulation of wild type *CCDC68* by two independent shRNAs increased tumor growth rate of MIAPaca-2 cells (Fig. 2C). All MIAPaca-2 shCCDC68 xenografts showed significantly increased tumor volumes and weights compared with the shLuc2 (luciferase control) tumors (Supplementary Fig. S2). Together these results indicate that *CCDC68* behaves as a TSG in PDAC xenografts.

CCDC68 protein expression is decreased in PDAC

We performed CCDC68 immunohistochemistry staining on tissue microarrays (TMA) created using 46 primary PDAC xenograft tissue specimens and several normal pancreas specimens. The normal interlobular and small duct epithelium consistently showed moderate cytoplasmic staining, but PDAC xenografts showed variable CCDC68 staining (Fig. 3A). Nearly 60% of PDAC cases showed lost/reduced CCDC68 protein expression as compared to normal ducts (Fig. 3A). CCDC68 was expressed in the supranuclear cytoplasm of normal duct epithelium (Fig. 3B) and well-differentiated PDAC (Fig. 3C), while significant loss of staining was evident in the moderately (Fig. 3D) and poorly differentiated PDAC (Fig. 3E).

Some CCDC68 staining was observed in the PDX stroma, however, this staining was not seen in either normal pancreas or human PDAC (Supplementary Fig. S3) and likely represents unspecific binding of CCDC68 antibody to protein expressed by mouse fibroblasts**.**

CCDC68 copy number loss occurs frequently in PDAC

To evaluate the role of gene deletion as a mechanism for loss of *CCDC68* expression, we assessed the copy number status of *CCDC68* in 19 PDAC cell lines and 32 patient-derived xenografts (PDX) models using a combination of qPCR and FISH analysis (Fig. 4A,B). FISH revealed loss of *CCDC68* DNA copy in 10/19 (50%) of PDAC cell lines analyzed (Supplementary Fig. S4). Since there was a correlation between qPCR and FISH analysis of *CCDC68* DNA copy number changes (Fig. 4A), we next assessed *CCDC68* DNA copy status in 32 PDX models using qPCR. DNA copy loss was defined as values below the mean +SD of qPCR derived DNA copy number in PDAC cell lines with two copies of *CCDC68* DNA by FISH. We documented *CCDC68* copy loss in 30% of PDX models (Supplementary Fig. S4).

To corroborate our finding of widespread copy number loss of *CCDC68* in PDAC, we analyzed copy number data from 125 primary PDAC donors made available by the International Cancer Genome Consortium (ICGC, project code PACA-AU). Nearly 50% of this cohort (60/125) exhibited copy number loss of the *CCDC68* gene. This rate of loss corresponded to a rank in the 91st percentile among all genes on chromosome 18, pointing to the specificity of this particular alteration in PDAC (Supplementary Fig. S5).

We next investigated the influence of copy number loss on *CCDC68* mRNA expression. mRNA expression was assessed by RT-qPCR covering two *CCDC68* exons in 32 primary patient-derived mouse xenograft (PDX) models and 19 PDAC cell lines with RT-qPCR analysis encompassing two *CCDC68* exons. There was no significant overall correlation between copy number and mRNA expression of *CCDC68* in PDAC xenografts and cell lines (Fig. 4B). However, there was an overall correlation between *CCDC68* mRNA and protein expression as determined in several PDAC cell lines (Fig. 4C) and PDX models (Fig. 4D).

Novel *CCDC68* alternate splice variant lacking amino acids 69–114

Although *CCDC68* copy number loss occurs in 50% of PDAC, only a small subset of those patients actually showed reduced *CCDC68* mRNA expression, suggesting additional regulatory mechanisms in PDAC. We hypothesized that mutation of *CCDC68* could account for loss of function in PDAC. Sequencing of *CCDC68* in 19 PDAC cell lines did not reveal any somatic mutations in *CCDC68*. However, in the AsPC-1 cell line we discovered a *CCDC68* transcript with deletion of exon 5 (Fig. 5A). To determine if this was caused by mutation in the splicing site, we amplified and sequenced the 5′donor splice site and indeed identified the c.620G>A substitution one nucleotide upstream of the exon 5 donor splice (SNP rs1344011) (Fig. 5B). PCR analysis revealed the presence of this SNP in 31% of PDX models (10/32) suggesting that its expression might be relevant to PDAC disease (data not shown). The translation analysis of rs1344011 *CCDC68* variant predicted a protein *CCDC68*$\Delta^{69–114}$ with histidine 69-lysine 114 in-frame deletion. This smaller

*CCDC68*Δ$^{69–114}$ protein was confirmed by western blotting in AsPC-1 as compared to 293T cells expressing exogenous *CCDC68*^{wt} and two cell lines, HPAF-II and MIAPaca-2 with high endogenous *CCDC68*^{wt} expression (Fig. 5C).

NetGene2 splice site prediction software revealed that G/A substitution in SNP rs1344011 decreases the strength of the donor splice site, suggesting that exon skipping may result from this substitution (http://www.cbs.dtu.dk/services/NetGene2/). To confirm this hypothesis, we subcloned minigene cassettes containing Exon5-Intron-Exon6 with (SNP) and without (wt) the rs1344011 substitution into the pET01 vector and overexpressed them in 293T and NIH3T3 cells. While cells transfected with either wt or SNP minigene Exon5-Intron-Exon6 cassette expressed the fused exon5-exon6 transcript, SNP minigene expressing cells also expressed a single exon6 transcript demonstrating the skipping of exon5 resulting from rs1344011 (Fig. 5D).

Our data indicates that while SNP rs1344011-containing AsPC-1 cells contain a single copy of *CCDC68* gene, both *CCDC68Δ*$^{69–114}$ and *CCDC68*^{wt} are expressed in these cells. This suggests that the rs1344011 splice donor substitution does not result in the complete skipping of exon 5 in *CCDC68* transcript. We hence sought to determine the ratio of the two *CCDC68* splice variants in PDAC cell lines and PDX models. First, H6c7 and AsPC-1 cells were subjected to RT-qPCR analysis using *CCDC68*Δ$^{69–114}$/*CCDC68*^{wt} specific primers (Fig. 5E), revealing that the rs13440011 variant accounts for ~40% of *CCDC68* transcripts in AsPC-1. We then tested 6 PDX models with detectable *CCDC68*Δ$^{69–114}$ mRNA expression and documented variable transcript ratios of *CCDC68*Δ$^{69–114}$/*CCDC68*^{wt} (Fig. 5F). Although variable ratios of *CCDC68*Δ$^{69–114}$/*CCDC68*^{wt} protein levels were also apparent in 6 PDX models (Fig. 5G) the levels did not correlate well with the *CCDC68*Δ$^{69–114}$/*CCDC68*^{wt} transcript levels suggesting that the levels of deleted and wild type *CCDC68* are regulated at the posttranscriptional level.

To address this discrepancy, we compared the protein stability of *CCDC68*^{wt} and *CCDC68*Δ$^{69–114}$ using a protein half-life assay in the presence of the protein translational inhibitor cyclohexamide. *CCDC68*Δ$^{69–114}$ showed significantly decreased half-life compared to *CCDC68*^{wt}, suggesting that loss of amino acids 69–114 impairs the protein stability of CCDC68 (Supplementary Fig. S6).

CCDC68 splice variant is non-functional as a tumor suppressor

We next investigated the “tumor suppressive” role of *CCDC68*Δ$^{69–114}$ variant in PDAC by overexpressing *CCDC68*^{wt} and *CCDC68*Δ$^{69–114}$ in PANC-1 cells and examined the effects on cellular proliferation (Supplementary Fig. S7), as well as subcutaneous and orthotopic tumor growth in *scid* mice (Fig. 6A,B). While overexpression of *CCDC68*^{wt} significantly decreased *in vivo* and *in vitro* growth of PANC-1 cells compared to the empty vector controls, this tumor suppressive effect was absent in PANC-1 cells expressing the truncated *CCDC68*Δ$^{69–114}$ (Fig. 6). These findings support the conclusion that the tumor suppressive properties of *CCDC68* are specific to the full-length isoform.

Discussion

Here we report the identification and demonstration of the tumor suppressive role of *CCDC68* in PDAC. We initially identified *CCDC68* in a screen for novel TSGs synergizing with *KRAS* oncogene to drive malignant transformation of a near-normal HPDE cell line and its tumor suppressive activity was confirmed in several PDAC cell line models. We showed that *CCDC68* loss of function occurs through copy number loss and the expression of an unstable protein isoform, $CCDC68\Delta^{69–114}$, which lack a tumor suppressive function.

Our initial analysis revealed *CCDC68* as a putative TSG whose loss of function enhanced tumor formation of H6c7-Kras cells in *scid* mice. Incomplete tumor penetrance of our *in vitro* PDAC H6c7 model (partly transformed by the *KRAS* oncogene) in *scid* mice prompted us to investigate the existence of additional genes that enhance the penetrance of this model as a result of acquired genomic alterations (6). Thus, we compared genomic profiles of partially penetrant H6c7-Kr cells with those of completely penetrant H6c7-KrasT cells to identify such candidates. aCGH analysis revealed prominent copy number losses on chromosomes 8p, 15p and 18q in H6c7-KrasT cell lines with 100% tumor penetrance. Integration of this genomic data with transcriptome data collected from both PDAC cell lines and patient samples identified *CCDC68* as the most probable candidate for enhancing the tumorigenesis of H6c7-Kr cells. This hypothesis was further strengthened by *in vitro* shRNA and cDNA screen that revealed *CCDC68* as a negative regulator of cell proliferation in H6c7-Kr, PANC-1 and MIAPaca-2 cell lines. This prompted us to continue investigation of *CCDC68* as a novel TSG in PDAC.

CCDC68 is located on the 18q chromosome arm frequently lost in PDAC. *SMAD4* has been recognized as a TSG in this region and is inactivated in 50% of PDAC by homozygous deletion or mutation. However, several studies have reported homozygous deletions (HDs) and loss of heterozygosity (LOH) in genes telomeric of the 18q21.1 locus (8–13). These include *ME2*, *ELAC1* and *MEX3C* on 18q21.1 and *DCC*, *SNORA37* and *MBD2* on 18q21.2. More recently, SNP analysis and exome sequencing has identified LOH and copy neutral LOH (CN-LOH) at the 18q resident genes *POLI* and *CCDC68* (3,13). Due to the high frequency of genetic alterations affecting genes located downstream of *SMAD4*, it is likely that other TSGs on 18q in PDAC remain to be identified. This hypothesis is strengthened by the observation that introduction of an additional copy of chromosome 18 into cultured PDAC cells decreases tumorigenic potential of these cells both *in vitro* and *in vivo* independently of *SMAD4* inactivation (14).

Our results indicated that 60% of PDAC patients have decreased *CCDC68* protein expression levels suggesting that the expression of *CCDC68* has negative effect on PDAC tumor biology. We also observed that *CCDC68* expression associates with well-differentiated tumors. However, since our cell line xenografts revealed no significant effect of *CCDC68* on overall differentiation it is not likely that *CCDC68* itself affects the differentiation status of PDAC tumors.

First line of evidence suggesting that CCDC68 might be a tumor suppressor was reported in colorectal adenocarcinoma where correlative copy number loss and CCDC68

underexpression was observed in majority of CRC patients (15). While, we documented copy loss of *CCDC68* in half of the PDAC cell lines and PDAC patients, no significant correlation between CCDC68 copy number and mRNA expression was observed. Mismatch between mRNA and copy number variation has been reported in cancer (16,17) and it reflects the numerous transcriptional regulatory mechanisms, including epigenetic and/or micro-RNA silencing. For CCDC68, this requires further investigations.

An additional novel and significant finding of our study is the identification of a novel *CCDC68* splice variant devoid of tumor suppressive function in PDAC. The truncated in-frame protein $CCDC68\Delta^{69–114}$ is a result of exon skipping in patients harboring a donor splice site variant SNP rs1344011. Specifically, we determined that: 1) wild type and splice variant transcripts are expressed in all SNP containing cell lines and tissues, independent of copy number; 2) PDAC patients carrying SNP rs1344011 exhibit a variable variant/wild type mRNA expression *CCDC68* ratio; 3) The $CCDC68^{wt}/CCDC68\Delta^{69–114}$ ratio appear to be regulated at the posttranscriptional level and 4) the protein isoform resulting from SNP rs1344011 has diminished tumor suppressive ability in PDAC cell lines. Disregulated alternative splicing plays a pivotal role in carcinogenesis. In the case of TSGs, induced overexpression of antagonistic variants in cancer is often phenotypically equivalent to loss of function and this has been shown for several tumor suppressors including *PTEN*, *BRCA1* and *TP53* (18–20). We demonstrated the absence of tumor suppressive activity of the *CCDC68* variant in PANC-1 cells, further suggesting that $CCDC68\Delta^{69–114}$ may functionally oppose $CCDC68^{wt}$. It remains to be investigated whether the *CCDC68* tumor suppressive function is regulated by a critical balance between wt and truncated variant *CCDC68* expression in patients carrying the rs1344011 SNP.

There was a mismatch between transcript and protein $CCDC68\Delta^{69–114}/CCDC68^{wt}$ ratios in tested PDX models suggestive of posttranscriptional regulation of CCDC68 variant levels. Several cellular mechanisms are in place to ensure the critical balance of particular proteins required for normal function including regulation of translation efficiency and protein turnover. In cancer including PDAC, this regulatory machinery is perturbed and would result in variant protein imbalances. Comparative experiments to investigate the protein stability $CCDC68^{wt}$ and $CCDC68\Delta^{69–114}$ show that the stability of *CCDC68* protein is in part dependent on amino acids 69–114. Hence, although PDX models 135 and 110 expressed high $CCDC68\Delta^{69–114}/CCDC68^{wt}$ transcript ratio levels, protein stability could account for decreased ratios of translated $CCDC68\Delta^{69–114}$ proteins. The variable $CCDC68\Delta^{69–114}/CCDC68^{wt}$ ratio across PDAC could then be explained by differences in the regulation of protein turnover.

In addition to differences in regulation, loss of aa69–114 could also impact the function of CCDC68 protein. Functional properties of proteins can be dramatically altered by a series of post-translational modifications (PTMs) that ultimately affect the chemical properties of proteins. Using PTM prediction tools, we have identified several putative PTMs including lysine acetylation, SUMOylation, O-linked glycosylation, phosphorylation and ubiquitination sites are residing in the aa69–114 of CCDC68 protein (Supplementary Fig. S8). The loss of any of these sites could have significant consequences on the function and/or regulation of *CCDC68*. However, further exploration of the cellular function(s) of

CCDC68 protein is needed to establish the impact of these PTMs on CCDC68 tumor suppressive ability.

This is the first study to describe a tumor suppressor role for *CCDC68* in cancer. Previous studies of *CCDC68* have been mainly descriptive. Originally named *se57-1*, *CCDC68* has been identified as a putative tumor antigen in 21% of cutaneous T-cell lymphoma (21), 17% of renal cell (22) and 15% of colorectal carcinoma patients (23). Simultaneously and consistent with our PDAC findings, the same studies documented dramatic losses of *CCDC68* expression in the majority of patients. Downregulation of *CCDC68* has also been documented in 89% of primary colorectal patients and its expression was highly correlated with the associated gene copy number (15). This data also suggests the possibility that *CCDC68* is also a novel candidate TSG in colorectal cancer. While this hypothesis requires further biological validation, the evidence of *CCDC68* loss of function in human malignancies is accumulating. TCGA catalogues *CCDC68* disruption through homozygous deletions, hypermethylation and somatic mutations across many human cancer types (http://www.cbioportal.org/). Our results on the role of *CCDC68* in pancreatic carcinogenesis and the accumulating evidence of *CCDC68* genetic alterations in cancer provide evidence that *CCDC68* is a putative tumor suppressor.

Materials and Methods

Cell culture

PDAC cell lines used in this study were obtained and cultured as recommended by the American Type Culture Collection (Manassas, VA). H6c7 cells were cultured as described previously (24).

Array comparative genomic hybridization

Tiling path arrays were processed as previously described (25). CGH profiles were segmented to identify DNA copy number alterations using aCGH-Smooth. Duplicate profiles for H6c7-Kr and H6c7-KrasT were compared and clones were only considered if they were altered in the same direction in both profiles. Resulting clones were compared between parental and derivative cell lines. Specific regions of gain and loss that spanned two or more adjacent clones were compiled for each derivative and genes mapping to within these altered regions were determined.

Microarray analysis

Transcriptional profiling was done using the Illumina HumanHT-12 v4 array (Illumina, San Diego, CA) and the data was processed as previously described (26). Genes were considered aberrantly expressed if the fold change between samples and controls exceeded 1.5-fold and expression differences common to all cell lines were included in subsequent analyses. A network consisting of human protein-protein interaction pairs was generated using MIMI Plugin in Cytoscape. Protein clusters representing highly interconnected regions in the network were generated using the MCODE plugin in Cytoscape.

Fluorescent in situ hybridization (FISH)

Two probes were used: internal control centromeric probe *CEP18* labeled with SpG (Abbott Molecular, Des Plaines, IL) and *CCDC68* (RP11-108F19 BAC clone probe; TCAG, Toronto, ON). The *CCDC68* probe was labeled with SpO using nick translation kit (Abbott Molecular) according to manufacturer's protocol and hybridization was performed as described previously (27). Slides were scored at 63x magnification on an Imager M1 Zeiss microscope (Carl Zeiss Canada Limited, Toronto, CA) and analyzed using the MetaSystems Isis FISH Imaging v5.3 (MetaSystems, Newton, MA). A minimum of 100 non-overlapping intact interphase nuclei were scored per each sample. 40% cut-off value was applied to identify a heterozygous loss of *CCDC68* in paraffin sections and 10% cut off value in cell suspensions.

Orfeome library and vector construction

Gateway *CCDC68* ORF entry clones obtained from Human ORFeome library Version 1.1 (Fisher Scientific, Ottawa, ON) were subcloned into the pLD-puro-Ccf and pLD-puro-tGFP (28) as described previously (29). All cell lines were STR genotyped and tested for mycoplasma.

Lentiviral shRNA knockdown

CCDC68 knockdown in MiaPACA-2 was accomplished using a lentiviral shRNA method with RNAi Consortium clones: shCCDC68-1; NM_025214.1-2062s1c1 (TRCN0000129087), shCCDC68-2; NM_025214.2-1313s21c1 (TRCN0000412383). The shRNA control used was shLUC2 (GTGCCAGAGTCCTTCGATTCC). Lentiviral transduction was performed using protocols from TRC (http://www.broad.mit.edu/rnai/trc/lib).

Mutation analysis

CCDC68 ORF was amplified from cDNA transcribed from normal H6c7 cells, 19 PDAC cell lines and 31 primary xenografts using Touchdown PCR (TD-PCR) as described previously (30). Generated PCR products (P2-F+P2-R primers) were subjected to direct sequencing using sequencing primers P2-SF and P2-SR (Supplementary TableS2). SNP was further confirmed with a new set of primers specifically amplifying the region in question.

Minigene assay

Genomic DNA from either H6c7 (WT) or AsPC-1 (SNP) including *CCDC68* intron-exon5-intron-exon6 was amplified using primers CCDC68DELFF and CCDC68151RR (Supplementary Table S2). The PCR fragment was subcloned into the pET01 exon trap vector (MoBiTec, Germany). After sequence confirmation, 293T and NIH3T3 cells were transfected with minigene constructs. RNA was isolated and the corresponding cDNA was amplified using pET01 specific forward primer (ETprim06) and CCDC68 reverse primer (P2SR). PCR products were examined on a 2% agarose gel.

Western analysis

Western analysis was described previously (31). Primary antibodies used in this study were: *CCDC68* (S1852; Epitomics, Burlingame, CA), *CCDC68* (SAB1103198;Sigma-Aldrich, St.Louis, MO) and β-*ACTIN* (A1978; Sigma Aldrich).

Immunohistochemistry (IHC)

IHC protocols were described previously (32). The staining intensity of CCD68 antibody (Sigma; SAB1103198,1:3000) was scored by a certified pathologist on a scale from 0–3 (0=absent; 1=low; 2=medium; 3=high).

DNA copy number analysis and RT-qPCR analysis

Quantitative polymerase chain reaction (qPCR) was performed as described previously (31) using two control genomic markers (G64212 and D4S1193) and two sets of *CCDC68* specific primers (P1-F+P2-D; 68QPCRLCM-F+68QPCRLCM-R). *CCDC68* copy number was estimated using comparative CT method relative to reference controls (n=3). Copy number changes were reported relative to median copy number changes across all the samples. Standard curve analysis was used or $CCDC68\Delta^{69-114}$ and $CCDC68^{wt}$ copy number estimation. cDNA was amplified using primers for $CCDC68^{w}$ (E6-7F1+R1) and $CCDC68\Delta^{69-114}$ (E4-6F1+R1). Standard curve was established using diluted vector DNA (pDONORCCDC68^{wt} and pDONORCCDC68Δ^{69-114}) ranging from 30–3 000 000 copies. RNA isolation and assay techniques were published previously (31). Relative quantification of qPCR data was performed using ΔΔCT method. The average Ct values for the duplicates were constructed separately for the target gene and two reference genes (*RPS13* and *β–ACTIN*). All the primers used are listed in Supplementary Table S2. Heatmaps were created using Integrative Genomic Viewer software (33).

xCELLigence and MTS assays

MTS assays were performed as described previously (31). Growth curves were constructed using the xCELLigence platform (ACEA Biosciences, San Diego, CA). Briefly, 5 000 cells were seeded per well of E-plate. Impedance was measured every 15 minutes for 120–144 hours.

Soft agar and tumorigenic assay

Soft agar assay was described previously (34). Tumorigenicity assay was performed in *scid* mice using subcutaneous and orthotopic injections as described (26) in accordance with protocols approved by the Animal Care Committee of the Ontario Cancer Institute.

Meta-analysis of DNA copy number and mRNA expression of PDAC patients

Copy number and mRNA expression profiling data from the Australian pancreatic cancer project (project code PACA-AU) was downloaded from the ICGC data portal (https://dcc.icgc.org). This study was chosen due to its large cohort size. Relevant data was extracted with custom parser scripts and manipulated and visualized using the R programming language.

Statistical analysis

All statistical analysis was performed using GraphPad Prism 5 (GraphPad, La Jolla, CA). Statistical tests used are indicated in each figure. P values <0.05 were considered significant.

Supplementary Material

Refer to Web version on PubMed Central for supplementary material.

Acknowledgments

We thank the following people for assistance: James Ho (IHC), Olga Ludkovksy (FISH) Ni Liu (PCR) and Dennis Wang (support in ICGC analysis).

Funding source: Supported by the Canadian Cancer Society Research Institute grant#700809, Canadian Institutes of Health Research grant MOP-49585, and the Ontario Ministry of Health and Long Term Care. N. Radulovich and K. Thu are Vanier Canada Graduate Scholars. Dr. S. Sakashita is supported by the Terry Fox Foundation STIHR Program in Molecular Pathology of Cancer at CIHR (STP 53912). Dr. Tsao is the M. Qasim Choksi Chair in Lung Cancer Translational Research.

References

1. Jemal A, Bray F, Center MM, Ferlay J, Ward E, Forman D. Global cancer statistics. CA Cancer J Clin. 2011; 61:69–90. [PubMed: 21296855]
2. Hruban RH, Maitra A, Goggins M. Update on pancreatic intraepithelial neoplasia. Int J Clin Exp Pathol. 2008; 1:306–316. [PubMed: 18787611]
3. Jones S, Zhang X, Parsons DW, Lin JC, Leary RJ, Angenendt P, et al. Core signaling pathways in human pancreatic cancers revealed by global genomic analyses. Science. 2008; 321:1801–1806. [PubMed: 18772397]
4. Campbell PJ, Yachida S, Mudie LJ, Stephens PJ, Pleasance ED, Stebbings LA, et al. The patterns and dynamics of genomic instability in metastatic pancreatic cancer. Nature. 2010; 467:1109–1113. [PubMed: 20981101]
5. Yachida S, Jones S, Bozic I, Antal T, Leary R, Fu B, et al. Distant metastasis occurs late during the genetic evolution of pancreatic cancer. Nature. 2010; 467:1114–1117. [PubMed: 20981102]
6. Qian J, Niu J, Li M, Chiao PJ, Tsao MS. In vitro modeling of human pancreatic duct epithelial cell transformation defines gene expression changes induced by K-ras oncogenic activation in pancreatic carcinogenesis. Cancer Res. 2005; 65:5045–5053. [PubMed: 15958547]
7. Thu KL, Radulovich N, Becker-Santos DD, Pikor LA, Pusic A, Lockwood WW, et al. SOX15 is a candidate tumor suppressor in pancreatic cancer with a potential role in Wnt/beta-catenin signaling. Oncogene. 2013
8. Bashyam MD, Bair R, Kim YH, Wang P, Hernandez-Boussard T, Karikari CA, et al. Array-based comparative genomic hybridization identifies localized DNA amplifications and homozygous deletions in pancreatic cancer. Neoplasia. 2005; 7:556–562. [PubMed: 16036106]
9. Nowak NJ, Gaile D, Conroy JM, McQuaid D, Cowell J, Carter R, et al. Genome-wide aberrations in pancreatic adenocarcinoma. Cancer Genet Cytogenet. 2005; 161:36–50. [PubMed: 16080956]
10. Kimmelman AC, Hezel AF, Aguirre AJ, Zheng H, Paik JH, Ying H, et al. Genomic alterations link Rho family of GTPases to the highly invasive phenotype of pancreas cancer. Proc Natl Acad Sci U S A. 2008; 105:19372–19377. [PubMed: 19050074]
11. Harada T, Chelala C, Crnogorac-Jurcevic T, Lemoine NR. Genome-wide analysis of pancreatic cancer using microarray-based techniques. Pancreatology. 2009; 9:13–24. [PubMed: 19077451]
12. Calhoun ES, Hucl T, Gallmeier E, West KM, Arking DE, Maitra A, et al. Identifying allelic loss and homozygous deletions in pancreatic cancer without matched normals using high-density single-nucleotide polymorphism arrays. Cancer Res. 2006; 66:7920–7928. [PubMed: 16912165]

13. Harada T, Chelala C, Bhakta V, Chaplin T, Caulee K, Baril P, et al. Genome-wide DNA copy number analysis in pancreatic cancer using high-density single nucleotide polymorphism arrays. Oncogene. 2008; 27:1951–1960. [PubMed: 17952125]
14. Lefter LP, Furukawa T, Sunamura M, Duda DG, Takeda K, Kotobuki N, et al. Suppression of the tumorigenic phenotype by chromosome 18 transfer into pancreatic cancer cell lines. Genes Chromosomes Cancer. 2002; 34:234–242. [PubMed: 11979557]
15. Sheffer M, Bacolod MD, Zuk O, Giardina SF, Pincas H, Barany F, et al. Association of survival and disease progression with chromosomal instability: a genomic exploration of colorectal cancer. Proc Natl Acad Sci U S A. 2009; 106:7131–7136. [PubMed: 19359472]
16. Ali Hassan NZ, Mokhtar NM, Kok Sin T, Mohamed Rose I, Sagap I, Harun R, et al. Integrated analysis of copy number variation and genome-wide expression profiling in colorectal cancer tissues. PLoS One. 2014; 9:e92553. [PubMed: 24694993]
17. Myhre S, Lingjaerde OC, Hennessy BT, Aure MR, Carey MS, Alsner J, et al. Influence of DNA copy number and mRNA levels on the expression of breast cancer related proteins. Mol Oncol. 2013; 7:704–718. [PubMed: 23562353]
18. Sharrard RM, Maitland NJ. Alternative splicing of the human PTEN/MMAC1/TEP1 gene. Biochim Biophys Acta. 2000; 1494:282–285. [PubMed: 11121587]
19. Hofstetter G, Berger A, Fiegl H, Slade N, Zoric A, Holzer B, et al. Alternative splicing of p53 and p73: the novel p53 splice variant p53delta is an independent prognostic marker in ovarian cancer. Oncogene. 2010; 29:1997–2004. [PubMed: 20101229]
20. Tammaro C, Raponi M, Wilson DI, Baralle D. BRCA1 exon 11 alternative splicing, multiple functions and the association with cancer. Biochem Soc Trans. 2012; 40:768–772. [PubMed: 22817731]
21. Eichmuller S, Usener D, Dummer R, Stein A, Thiel D, Schadendorf D. Serological detection of cutaneous T-cell lymphoma-associated antigens. Proc Natl Acad Sci U S A. 2001; 98:629–634. [PubMed: 11149944]
22. Devitt G, Meyer C, Wiedemann N, Eichmuller S, Kopp-Schneider A, Haferkamp A, et al. Serological analysis of human renal cell carcinoma. Int J Cancer. 2006; 118:2210–2219. [PubMed: 16331622]
23. Gerhardt A, Usener D, Keese M, Sturm J, Schadendorf D, Eichmuller S. Tissue expression and sero-reactivity of tumor-specific antigens in colorectal cancer. Cancer Lett. 2004; 208:197–206. [PubMed: 15142679]
24. Furukawa T, Duguid WP, Rosenberg L, Viallet J, Galloway DA, Tsao MS. Long-term culture and immortalization of epithelial cells from normal adult human pancreatic ducts transfected by the E6E7 gene of human papilloma virus 16. Am J Pathol. 1996; 148:1763–1770. [PubMed: 8669463]
25. Lockwood WW, Chari R, Chi B, Lam WL. Recent advances in array comparative genomic hybridization technologies and their applications in human genetics. Eur J Hum Genet. 2006; 14:139–148. [PubMed: 16288307]
26. Leung L, Radulovich N, Zhu CQ, Wang D, To C, Ibrahimov E, et al. Loss of Canonical Smad4 Signaling Promotes KRAS Driven Malignant Transformation of Human Pancreatic Duct Epithelial Cells and Metastasis. PLoS One. 2013; 8:e84366. [PubMed: 24386371]
27. Hirsch FR, Varella-Garcia M, Bunn PA Jr, Di Maria MV, Veve R, Bremmes RM, et al. Epidermal growth factor receptor in non-small-cell lung carcinomas: correlation between gene copy number and protein expression and impact on prognosis. J Clin Oncol. 2003; 21:3798–3807. [PubMed: 12953099]
28. Mak AB, Ni Z, Hewel JA, Chen GI, Zhong G, Karamboulas K, et al. A lentiviral functional proteomics approach identifies chromatin remodeling complexes important for the induction of pluripotency. Mol Cell Proteomics. 2010; 9:811–823. [PubMed: 20305087]
29. Radulovich N, Leung L, Tsao MS. Modified gateway system for double shRNA expression and Cre/lox based gene expression. BMC Biotechnol. 2011; 11 24-6750-11-24.
30. Don RH, Cox PT, Wainwright BJ, Baker K, Mattick JS. ‘Touchdown’ PCR to circumvent spurious priming during gene amplification. Nucleic Acids Res. 1991; 19:4008. [PubMed: 1861999]
31. Radulovich N, Pham NA, Strumpf D, Leung L, Xie W, Jurisica I, et al. Differential roles of cyclin D1 and D3 in pancreatic ductal adenocarcinoma. Mol Cancer. 2010; 9:24. [PubMed: 20113529]

32. Navab R, Liu J, Seiden-Long I, Shih W, Li M, Bandarchi B, et al. Co-overexpression of Met and hepatocyte growth factor promotes systemic metastasis in NCI-H460 non-small cell lung carcinoma cells. Neoplasia. 2009; 11:1292–1300. [PubMed: 20019837]

33. Thorvaldsdottir H, Robinson JT, Mesirov JP. Integrative Genomics Viewer (IGV): high-performance genomics data visualization and exploration. Brief Bioinform. 2013; 14:178–192. [PubMed: 22517427]

34. Ouyang H, Mou L, Luk C, Liu N, Karaskova J, Squire J, et al. Immortal human pancreatic duct epithelial cell lines with near normal genotype and phenotype. Am J Pathol. 2000; 157:1623–1631. [PubMed: 11073822]

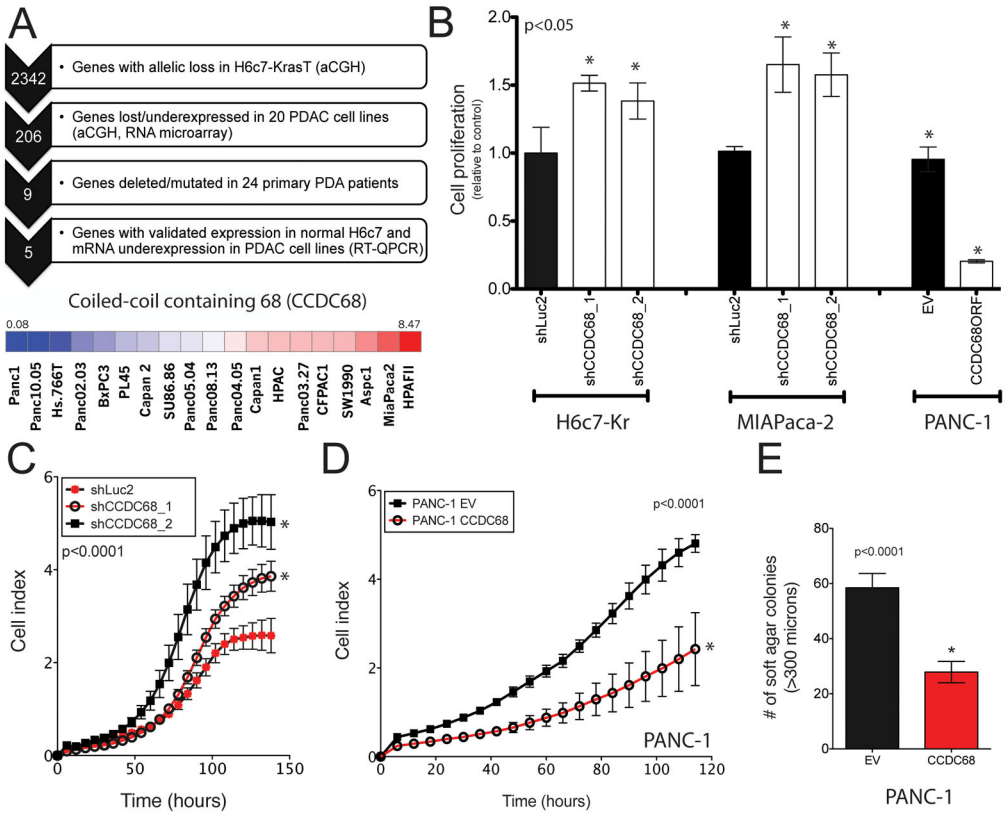

Figure 1. *In vitro* proliferation screen identifies *CCDC68* as a putative TSG in PDAC

A. Flow diagram of the integrative genomic analysis utilized for the identification of putative tumor suppressor genes in PDAC. Bottom panel is the HeatMapViewer displaying average *CCDC68* mRNA expression values across PDAC cell lines relative to H6c7 as measured by three independent RT-qPCR experiments. The largest expression values are shown as red bars and the smallest values are displayed as blue bars. **B.** The changes in cell proliferation as a result of *CCDC68* overexpression or knockdown were measured 72 hour post transfection using MTS proliferation assay. The bars represent mean±SD of four replicates. $p<0.05$; One-way ANOVA, Bonferroni. **C.** Stable knockdown of *CCDC68* in MIAPaca-2 cells significantly increased their growth. **D.** Stable overexpression of *CCDC68* in PANC-1 cell line significantly decreased their growth as measured by XCELLigence. The data points (**C, D**) represent mean±SD for two independent experiments. $p<0.0001$; ANOVA-mixed model, Bonferroni. **E.** Graph enumerating soft agar colony formation of PANC-1 EV and PANC-CCDC68 cells. Data denotes mean±SD of three independent experiments. $p<0.0001$ Student t test.

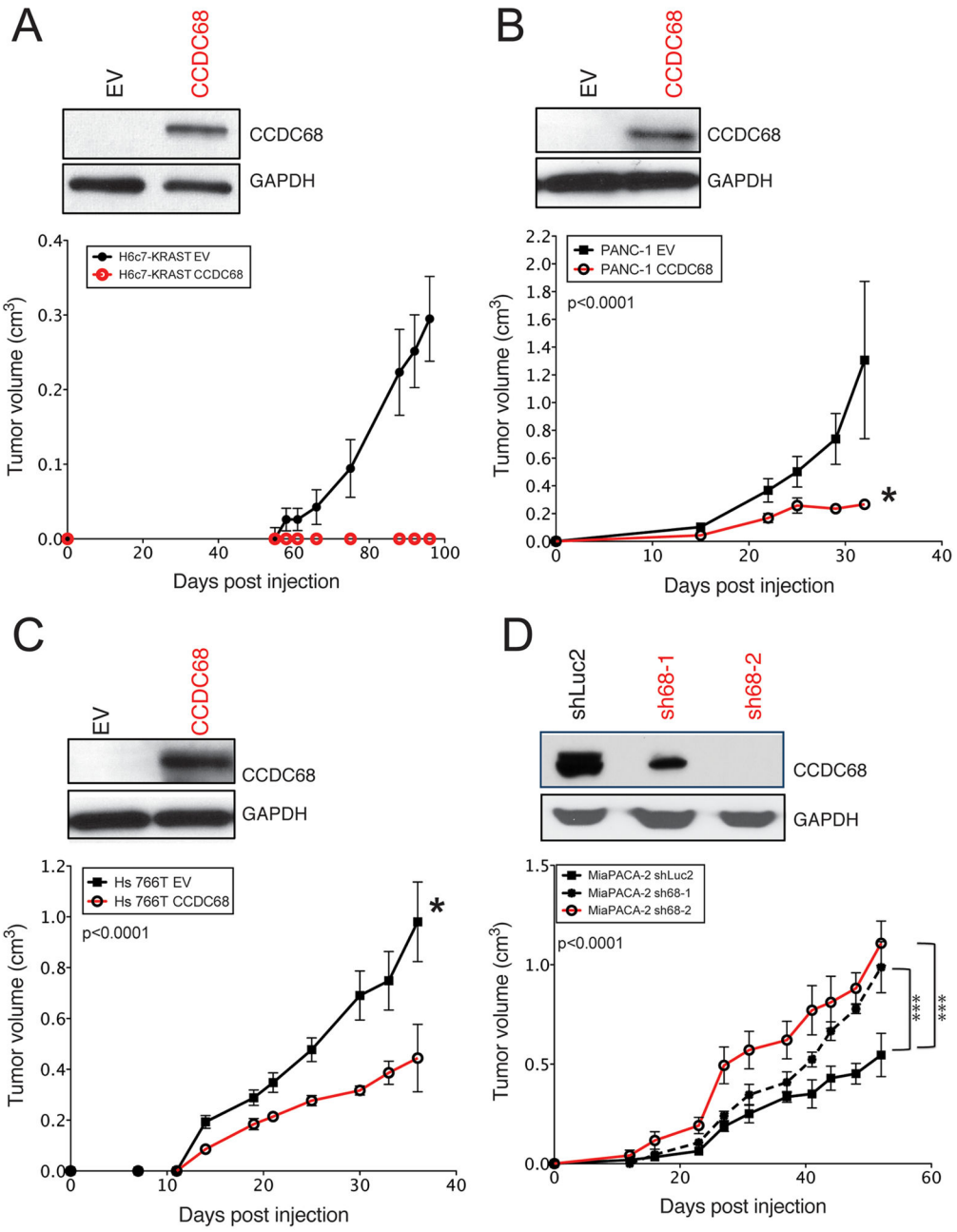

Figure 2. *CCDC68* mediates tumorigenicity in *scid* mice

CCDC68 was stably overexpressed in **A.** H6c7-KrasT, **B.** PANC-1 A. and **C.** Hs.766T, and downregulated in **D.** MIAPaca-2 cell lines. Resulting cell lines and their controls were then injected in *scid* mice and tumor growth was monitored over time. Data points represent mean±SD of tumor measurements in 5 animals. p<0.0001, Mixed-model ANOVA, Bonferroni.

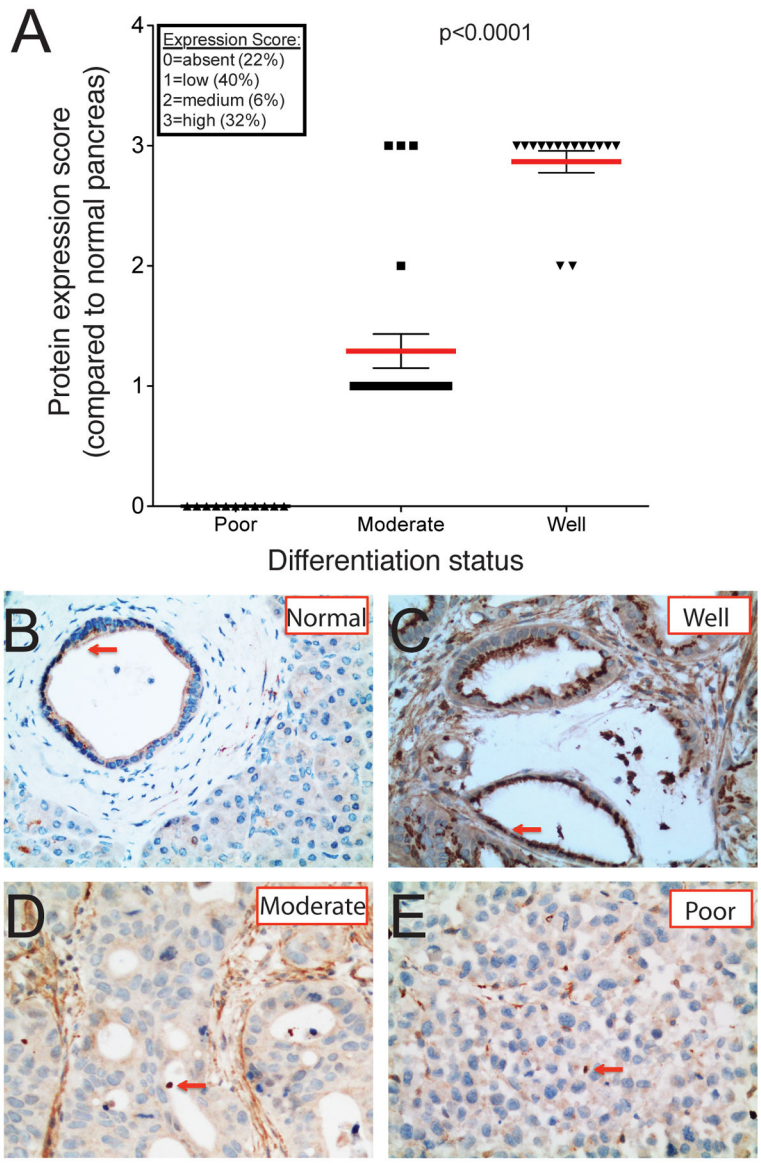

Figure 3. *CCDC68* protein expression is associated with differentiation status in PDAC

(A) IHC was performed on TMA for 46 PDAC xenografts and normal pancreas using a CCDC68 specific antibody optimized for IHC. The graph summarizes the scoring results of all TMAs as compared to expression in normal pancreatic ducts. p<0.0001, Mann-Whitney U. *CCDC68* perinuclear expression was apparent on the apical side of the normal pancreatic ducts (**B)** and well-differentiated tumors **(C)**. Moderately (**D)** and poorly (**E)** differentiated tumors showed random and low expression of *CCDC68* protein.

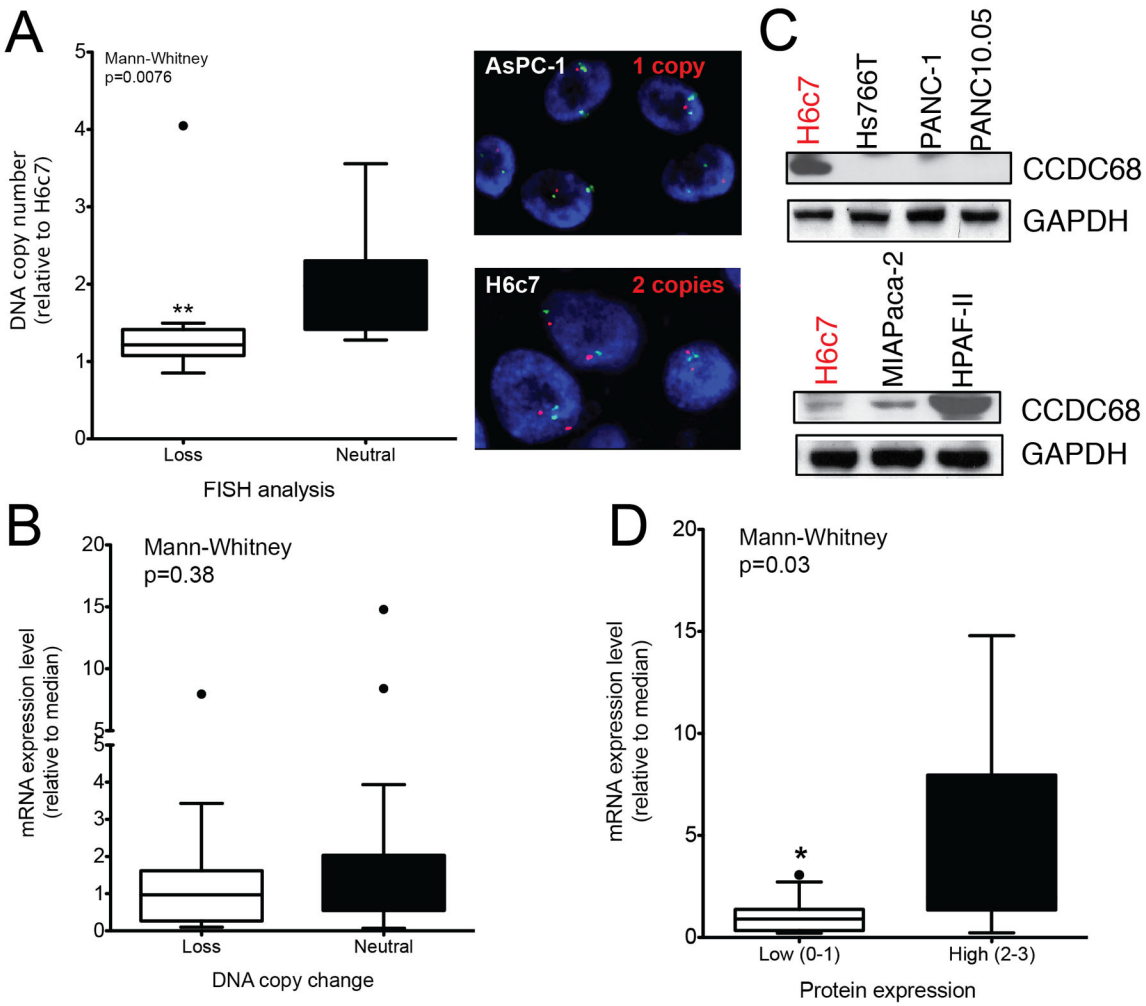

Figure 4. *CCDC68* copy number status and mRNA expression in PDAC

(A) The loss of *CCDC68* DNA copy number was documented in 19 PDAC cell lines using FISH and qPCR analysis. Cell lines were divided into two groups based on the status of *CCDC68* copy number as determined by FISH. Images are showing the DNA copy loss of *CCDC68* in representative cell lines as revealed by FISH analysis. **(B)** Correlation analysis of *CCDC68* DNA copy number and *CCDC68* mRNA expression in 32 primary xenografts and 19 cell lines measured using qPCR. The data represent averages of three independent experiments for each sample. **(C)** Western blotting using *CCDC68* specific antibody confirms the mRNA expression changes in selected PDAC cell lines. **(D)** Correlation of *CCDC68* mRNA levels with *CCDC68* protein levels in PDX models. Protein expression was scored by IHC while mRNA expression was measured using qPCR. Average data in **A)**, **B)** and **D)** was plotted for each sample and represented by the Tukey boxplot. p value is calculated using Man-Whitney statistical test.

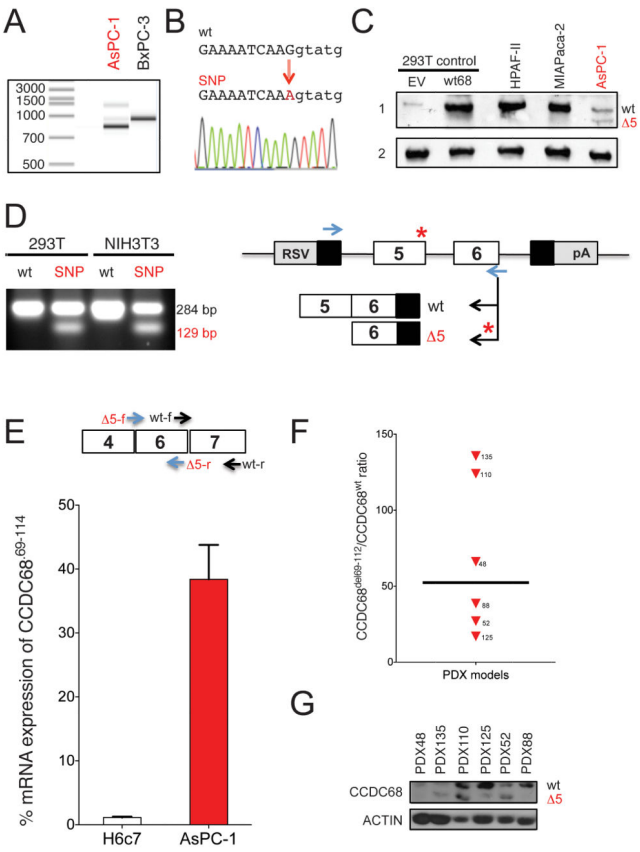

Figure 5. Identification of novel *CCDC68*Δ$^{69–114}$ splice variant

(**A)** Amplification of full length *CCDC68* ORF by PCR shows truncated PCR fragment in AsPC-1 cells. (**B)** Chromatogram demonstrating the G-A substitution occurring in exon 5 donor splice site in AsPC-1 cell line DNA. (**C)** Endogenous protein expression of truncated AsPC-1 CCDC68 protein. 293T protein lysate was isolated 72 hours following transient transfection of 293T cells with either EV or pENTR-CCDC68 vector expressing full length *CCDC68*^{wt} cDNA. 1=CCDC68, 2=actin loading control. (**D)** Minigene analysis confirms the exon 5 skipping as a result of SNP r.1344011 variation. Red stars show the position of SNP rs.1344011 in the minigene construct. E) *CCDC68*Δ$^{69–114}$ specific mRNA expression was documented in AsPC1 cells using q-RT-PCR as outlined in the Materials and Methods. Data points represent mean±SD from two independent experiments. Variable ratios of *CCDC68*Δ$^{69–114}$/*CCDC68*^{wt} mRNA **(F)** and protein **(G)** levels were documented in PDX models. Data points in F) represent means of three independent experiments.

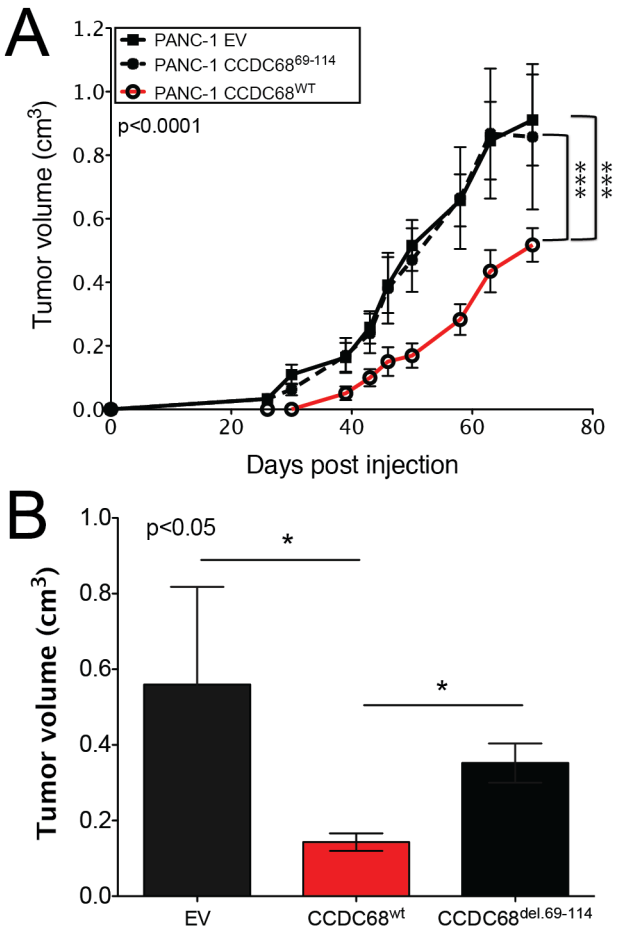

Figure 6. Loss of amino acids 69-114 decreases the tumor suppressive function of CCDC68

PANC-1 cells expressing EV, *CCDC68*^{wt} or *CCDC68*$\Delta^{69–114}$ were implanted **(A)** subcutaneously or **(B)** orthotopically into the pancreas of *scid* mice. **(A)** Data points represent mean±SE of tumor measurements in 5 animals over time. $p<0.05$; Mixed-model ANOVA, Bonferroni **(B)** Pancreatic tumors were removed 30 days post implantation and the data points represent mean^{+} SE of final tumor volumes in 5 mice. $p<0.05$;Two-way ANOVA; Bonferroni).